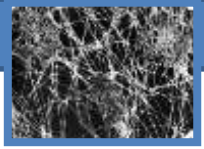

# Plateauova – Rayleighova nestabilita
# Rozpad kapalinové trysky

**David Lukáš**

a

Doc. Ing . Eva Kuželová Košťáková, Ph.D.
Katedra chemie, FP, TUL
Eva.kostakova@tul.cz
Tel.: 48 535 3489
Budova C, 3. patro

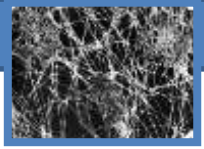

## *Rayleigh-Plateau Instability*: Falling Jet - Princeton University

Rayleigh-Plateau Instability:
Falling Jet Analysis and Applications
Oren Breslouer
MAE 559
1/08/10
Final Project Report

http://www.princeton.edu/~stonelab/Teaching/Oren%20Breslouer%20559%20Final%20Report.pdf

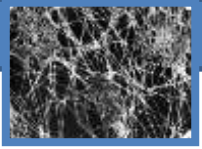

# Výroba základní vlákenné vrstvy přímo pod tryskou

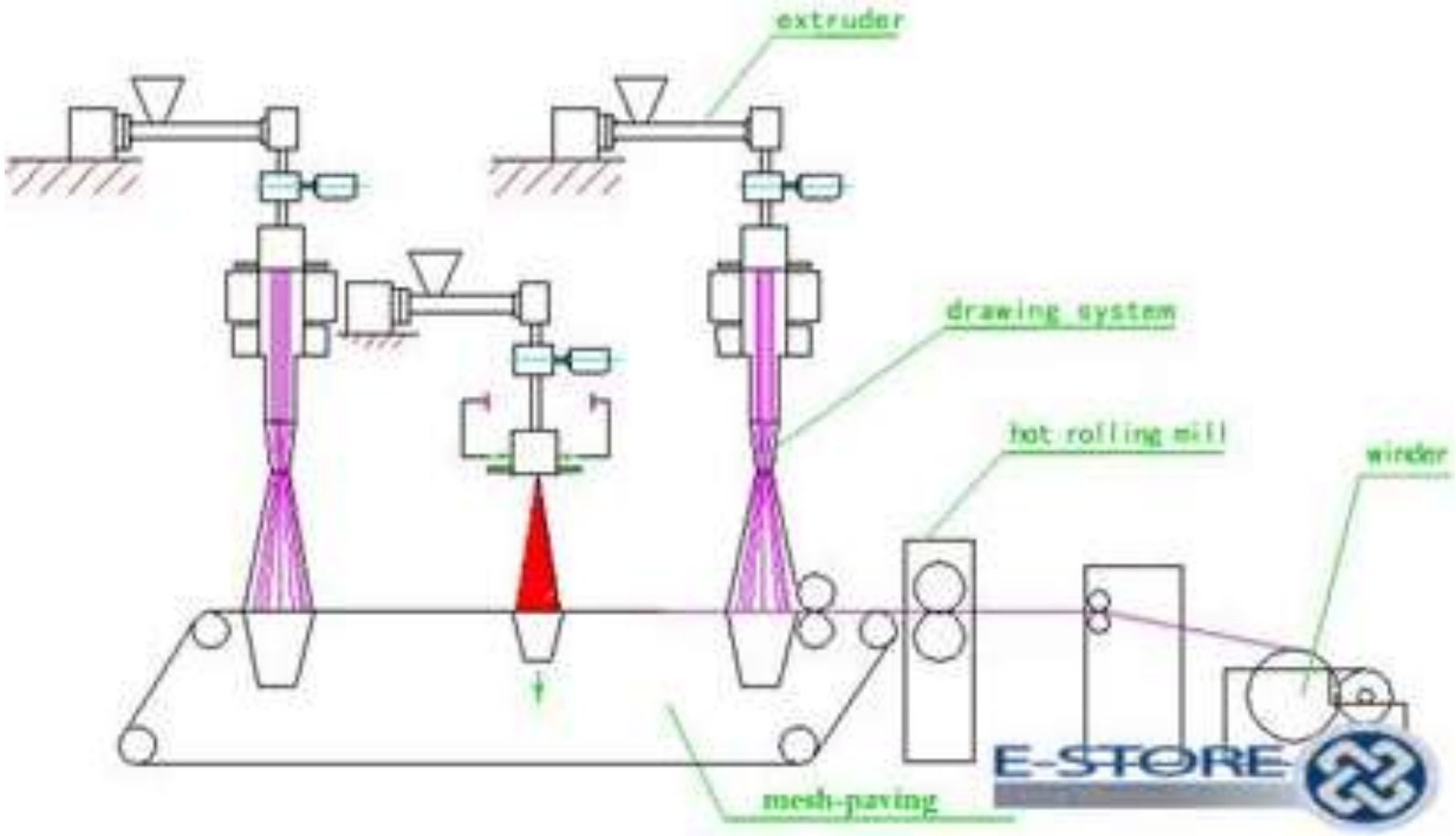


Spunbond ,*meltblown* a *elektrostatické zvlákňování* jsou technologiie výroby netkaných textilií **přímo z polymeru**.

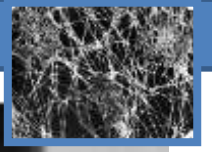

**Video:**

http://www.youtube.com/watch?v=UYRGEINpO50

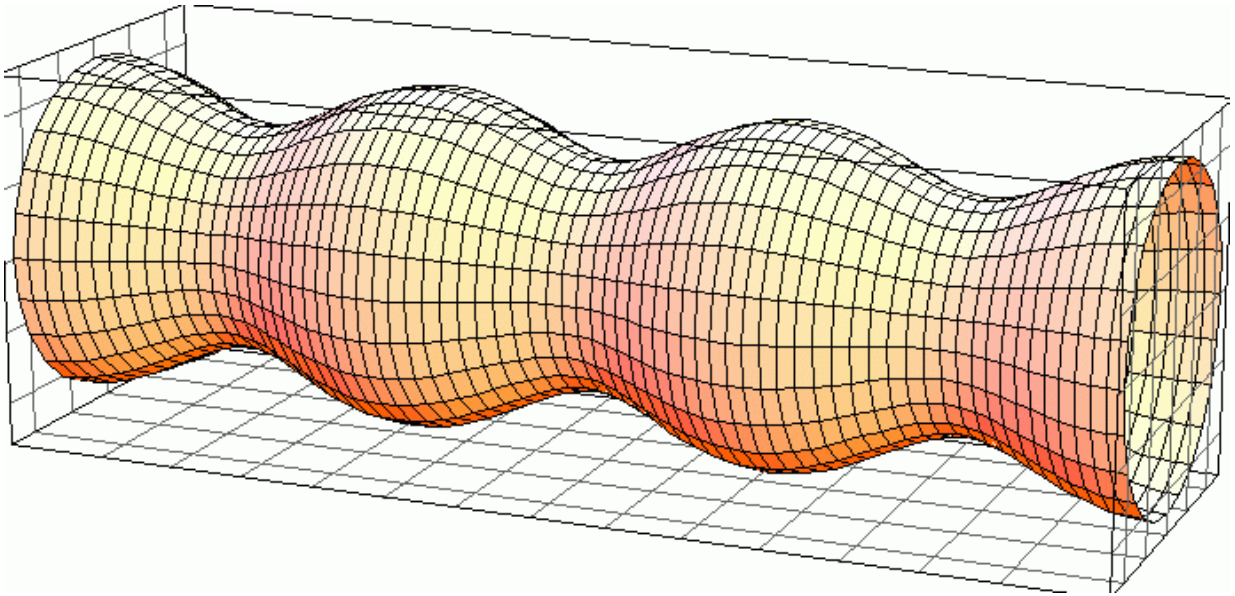

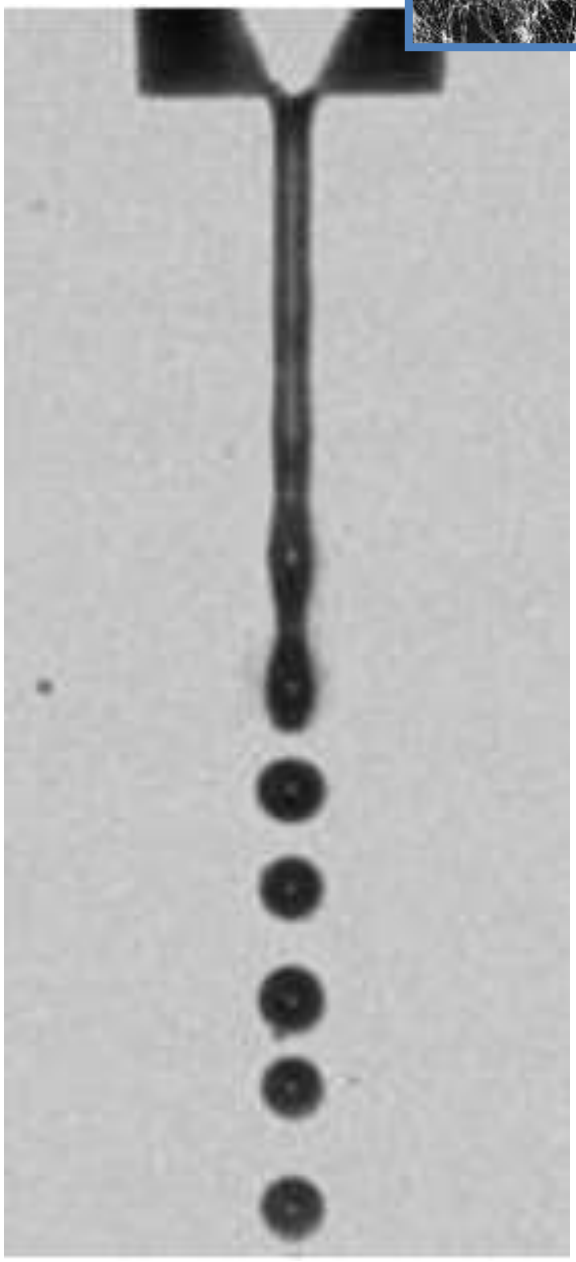

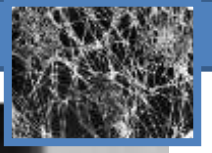

## Kvalitativní popis Plateau-Rayleighovy nestability

A liquid jet, initially of constant radius *r*, is falling vertically under gravity.

The liquid length *L* increases and reaches a critical value.

At this critical value , *L*, the jet loses its cylindrical shape as it decomposes into a stream of droplets.

This phenomenon occurs primarily as a result of surface tension.

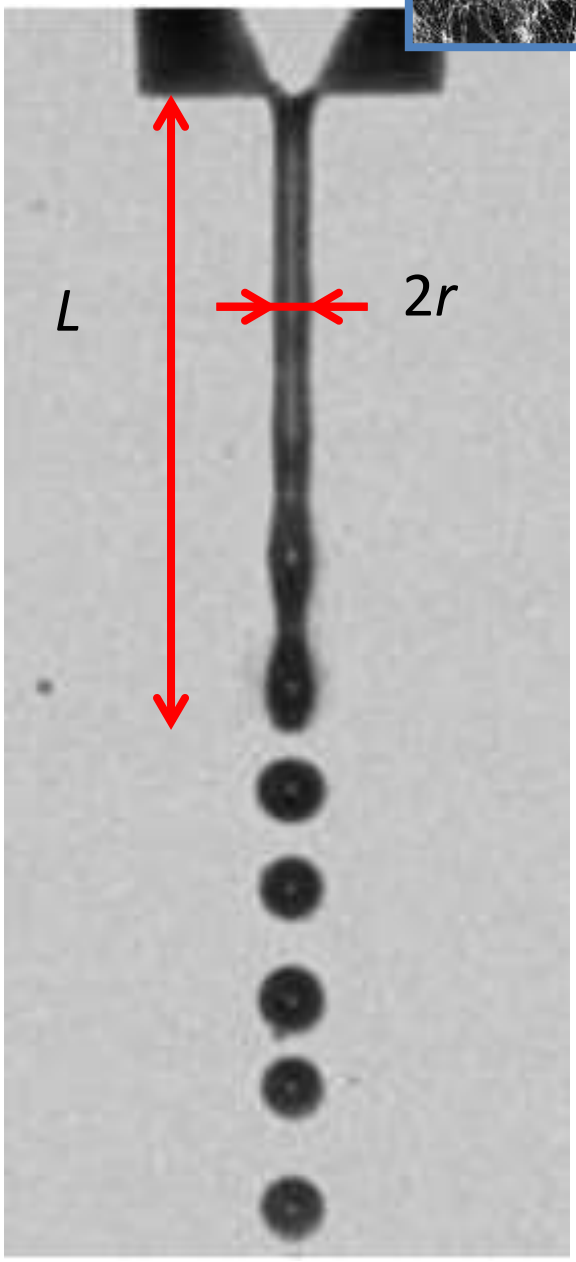

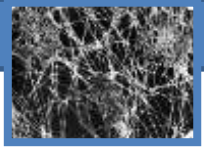

Joseph Plateau first characterized this instability in 1873 through experimental observation, building on the work of Savart.

He noted the instability arose when the liquid column length exceeded the column diameter by a factor of about 3.13.

$$\lambda = 2\pi r$$

**Joseph Antoine Ferdinand Plateau** was a Belgian physicist.

Daguerrotype portrait of Belgian physicist Joseph Plateau dated 1843

http://en.wikipedia.org/wiki/Joseph_Plateau

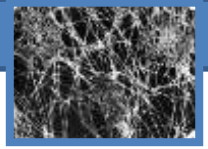

Lord Rayleigh later corroborated Plateau's work, giving an analytical explanation of this physical observation.

**John William Strutt, 3rd Baron Rayleigh**, (12 November 1842 – 30 June 1919) English physicist .

He discovered **argon**, for what he earned the Nobel Prize for Physics in 1904.

http://en.wikipedia.org/wiki/John_Strutt,_3rd_Baron_Rayleigh

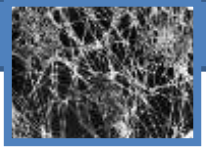

Plateau-Rayleigh instability derives from the existence of small perturbations in ar physical system.

All real-world flows have some non-negligible external disturbance that will increase exponentially in unstable systems.

In general, this deformation of the column, called *varicose perturbations, is represented as a series of periodic displacement sinusoids*.

For certain wavelengths, these perturbation waves will grow larger in time.

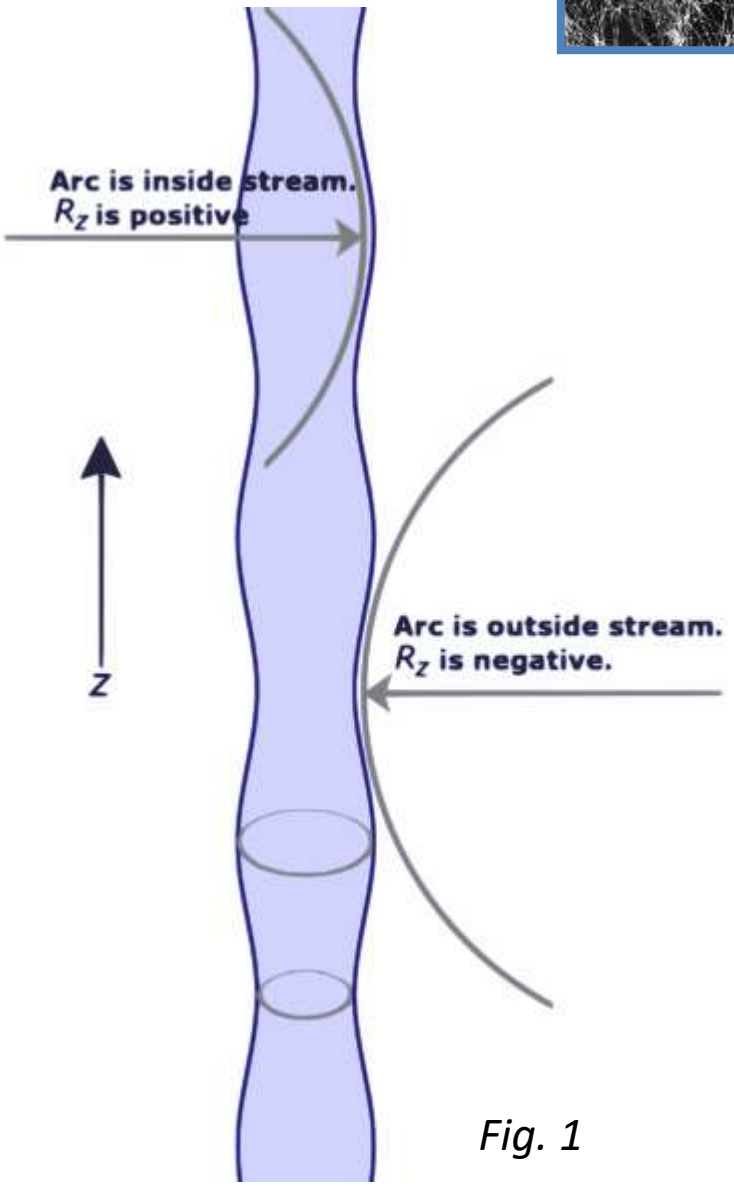


*Fig. 1*

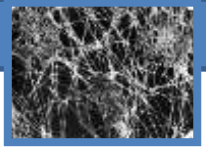

As the amplitude of the displacement grows, the liquid column will no longer have a constant radius of curvature.

Within short times, or small lengths, the jet is a cylinder with curvatures

$$K_1 = \frac{1}{r}, \quad K_2 = 0$$

The perturbed cylinder has areas with ???positive curvature and other areas with negative curvature???.

From Young - Laplace,

$$p = \gamma\left(K_1 + K_2\right)$$

Pinched sections have higher pressure (1/*R is greater)*

*and the bulging sections have* lower pressure, thereby producing a fluid flow due to pressure gradient.

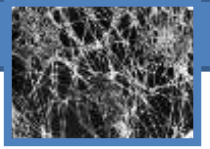

This internal flux causes the growth of displacement amplitude which eventually initiates droplet formation.

The droplets form when the pinched areas rupture.

As with all surface tension dominated problems (compressibility and viscous forces are negligible).

The specific system geometry depends on energy minimization. A liquid "desires" to be in a minimal energy state.

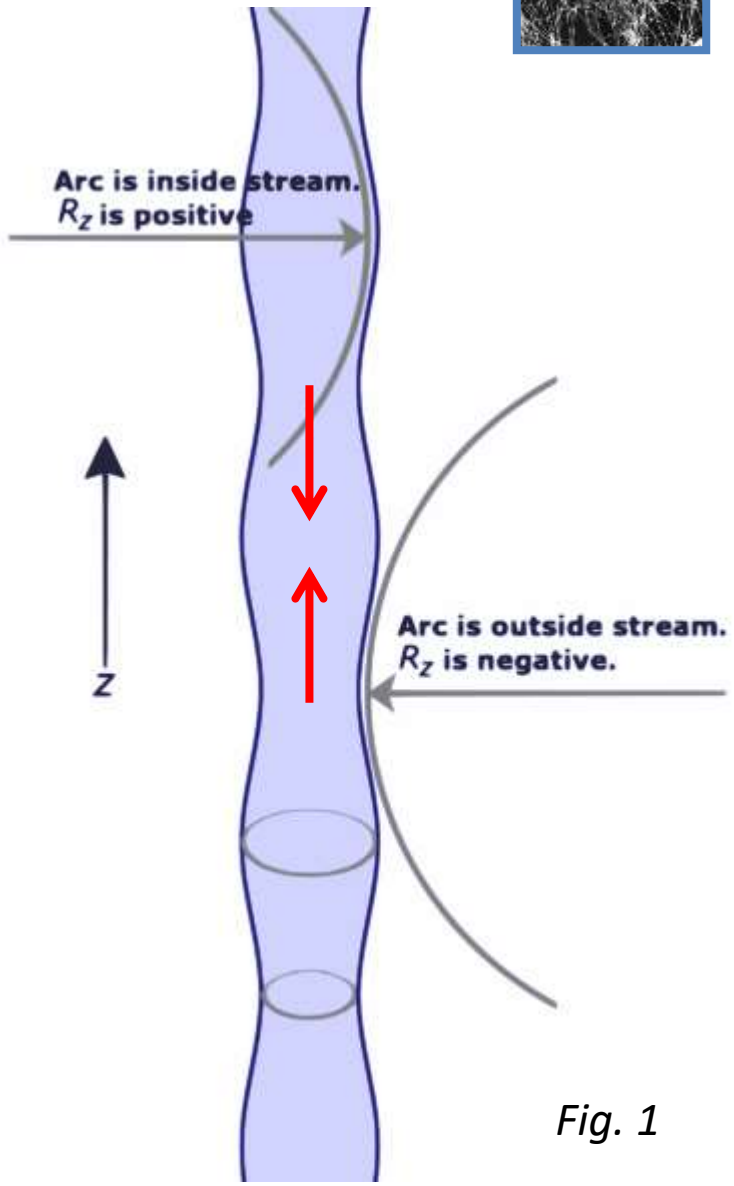


*Fig. 1*

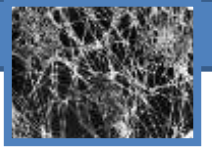

A lower energy state, a result of a total decreased surface area, exists if the fluid breaks into droplets.

(flickr.com/photos/sqlnerd/204436953/) and Fig. 3 (Hagedorn, 2004) for representational images of the instability.

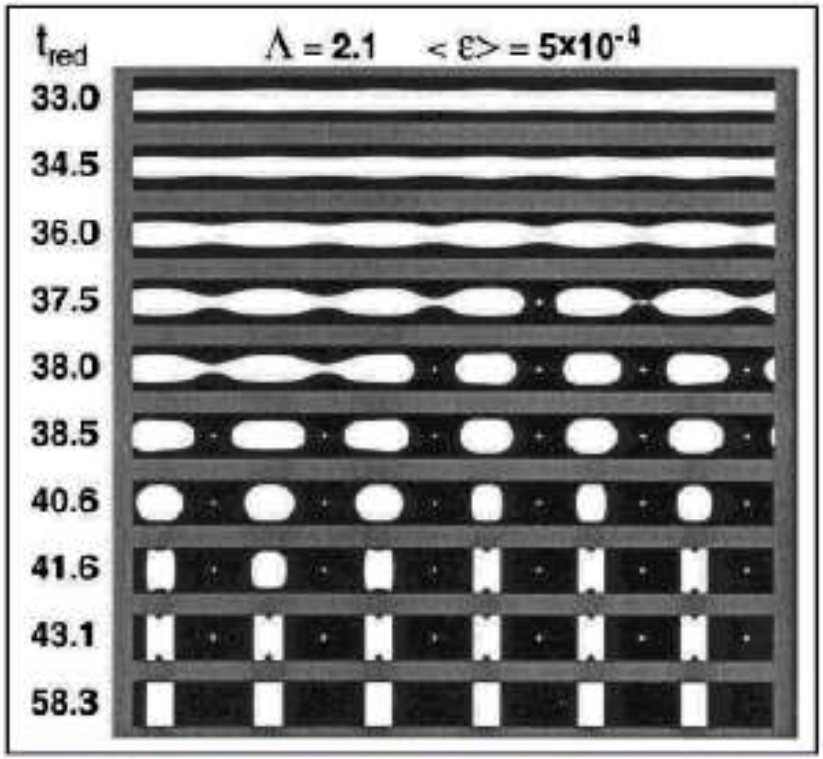


Figure 3: Numerical simulation of instability in horizontal liquid column

Fig. 2


Fig. 3

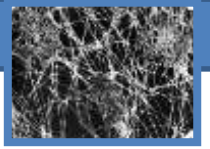

$$\mathrm{Re} = \frac{\text{inertial forces}}{\text{viscous forces}} = \frac{\rho \mathbf{v} L}{\mu} = \frac{\mathbf{v} L}{\nu}$$

$$V \cong 5 m/s \qquad L = r \cong 10^{-3} m$$

$$\nu \cong 0.7 Pa\,s \cdot 10^{-3} m \qquad \text{Re= 71,4}$$

Viscosity and gravity effects (thinning) are neglected per the assumption of insignificant viscous forces (high Re number).

Rayleigh concludes, “In the cases just considered, the cause of the instability is statical, and the phenomena are independent of the general translatory motion of the jet.” (Rayleigh, 1878)

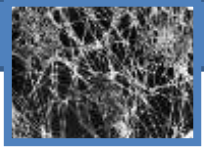

| Substance | Viscosity (Pa·s $10^{-3}$) | Temperature (°C) |
|---|---|---|
| Benzene | 0.604 | 25 |
| Water[63] | 1.0016 | 20 |
| Mercury | 1.526 | 25 |
| Whole milk[64] | 2.12 | 20 |
| Olive oil[64] | 56.2 | 26 |
| Honey[65] | 2000-10000 | 20 |
| Ketchup[a][66] | 5000-20000 | 25 |
| Peanut butter[a][67] | $10^4$-$10^6$ | |
| Pitch[62] (Smola) | $2.3\times10^{11}$ | 10-30 (variable) |

https://en.wikipedia.org/wiki/Viscosity

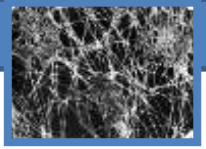

## Motivace pro výzkum P-R nestability a aplikace

Lord Rayleigh's initial interest in the problem seems to be wholly academic.

He begins his seminal paper, "It may even be said, most of the still unexplained phenomena of Acoustics are connected with the instability of jets of fluid". (*„Je dokonce možné říci, že většina dosud nevysvětlených jevů akustiky je spojena s nestabilitou proudů tekutin".*)

The system represents one of many examples of dynamic surface tension fluid flows. The relatively simple experimental results give rise to a rigorous mathematical representation that robustly explains the underlying phenomena.
Systém představuje jeden z mnoha příkladů dynamických toků tekutin povrchového napětí. Relativně jednoduché experimentální výsledky dávají vzniknout rigorózní matematické reprezentaci, která důkladně vysvětluje základní jevy.

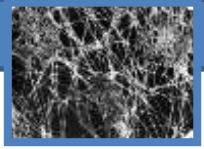

The problem also has analogues to other fluid flow problems. First, similar analysis is appropriate for a thin film coating a cylindrical rod or fiber. This fluid film is inherently unstable and the growth of perturbations mirrors that of the Rayleigh-Plateau instability. In this formulation, viscous effects and the hydrophillicity of the wetted material become important but the general behavior, where a cylindrical column of liquid devolves into a series of droplets, is identical.

Electrospinning

www.phys.ens.fr

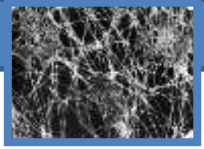

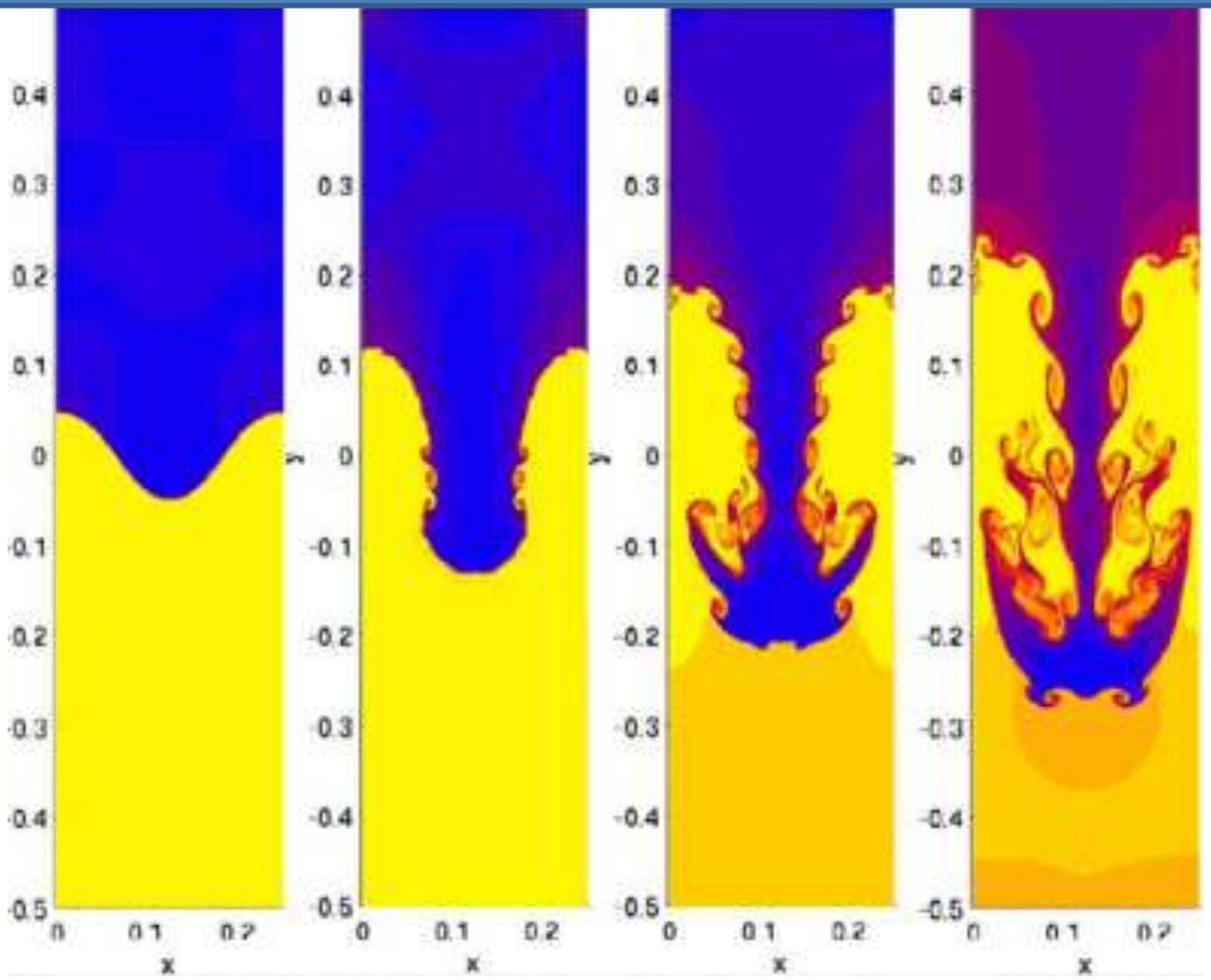


Core-shell electrospinning

Second, it is related to the Rayleigh-Taylor instability which occurs between two immiscible and parallel fluids of unequal density.

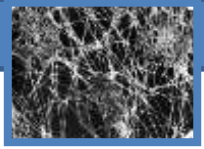

Third, The number of droplets of the crown splash (occurring following a droplet impact into a stationary liquid layer) is determined by the longest wavelength of the Rayleigh-Plateau instability. The splashing rim can be modeled as an unstable cylinder subject to the instability (Deegan, 2008).

media.efluids.com

Video:
http://www.youtube.com/watch?v=NVeswxAVRvc

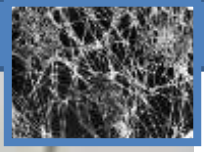

Lukáš, D., Sarkar, A., Martinová, L., Vodsed'álková, K., Lubasová, D., Chaloupek, J., Pokorný, P., Mikeš, P., Chvojka, J. and Komárek, M. (2009)'Physical principles of electrospinning (Electrospinning as a nano-scale technology of the twentyfirst century)',*Textile Progress*, 41:2,59 — 140



*Figure 3.8. The self-organisation of jets on a free liquid surface is qualitatively illustrated using a motion of a droplet of a very viscous component of epoxy resin under increasing external field strength. The droplet is deposited on a bulky metallic rod of diameter slightly greater than one centimetre that serves as an electrode in an electrospinner. A collector is placed at an upper level, outside the depicted zone. At zero field strength the viscous droplet has a hemispherical shape, as shown in the left hand side of the figure. Above the critical field intensity value liquid jets are self-organized, shown in the most right hand side of the figure. (Courtesy of Sandra Torres, Technical University of Liberec)*

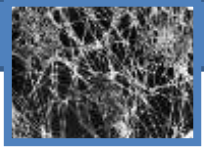

Another, rather surprising, analogous problem involves the stability of spacetime. A black hole is stretched along some arbitrary dimension into a "black string" and then perturbed along this dimension. It is hypothesized that the black string will breakup into smaller black holes, as in the Rayleigh-Plateau instability. Instead of surface tension and fluid fields such as pressure and velocity, the system is governed by Einstein's general relativity equations, gravity,
and other cosmological phenomena (Cardoso, 2006).

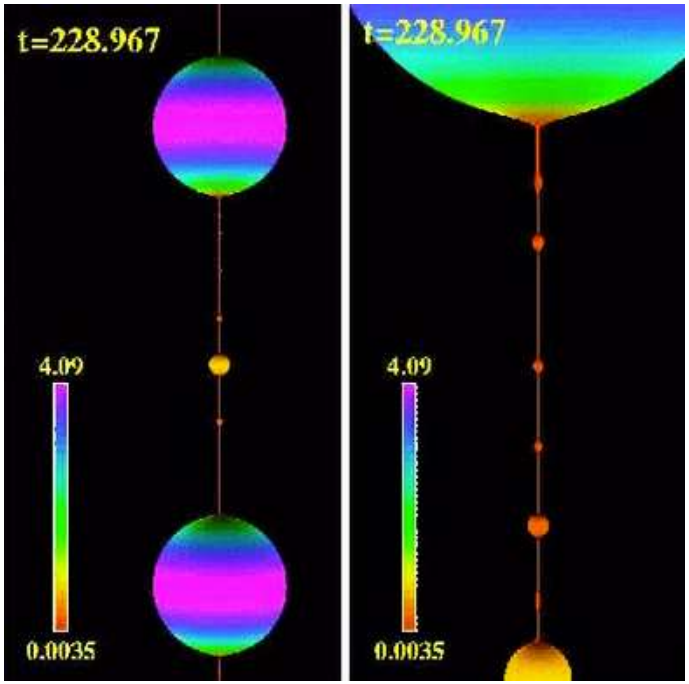


This animation shows a black string evolving into black holes connected by thin string segments. Smaller black holes form on the unstable string segments, resulting in a cascade that leads to a naked singularity before ending as a black hole. Credit: Frans Pretorius.

Read more at:
http://phys.org/news203318795.html#jCp

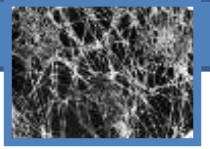

The most common application is in inkjet printing.

The inkjet stream breaks into extremely small droplets, on the order of 50 □m, tha flow at a regular interval in accordance wit Rayleigh-Plateau.

Most inkjet printers initiate the instability with pressure or thermal perturbations.

Behind the ink nozzle, subsequently giving each droplet a charge that determines its deflection onto the paper matrix.

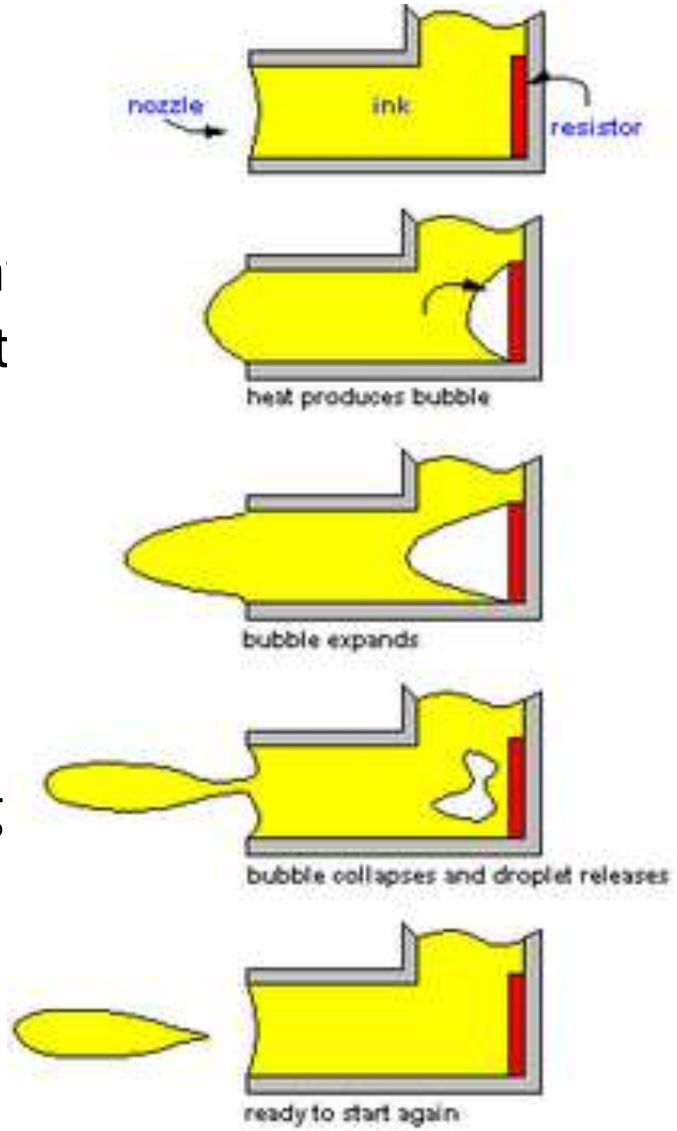

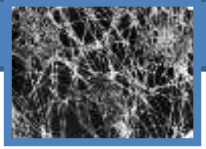

"Lab on a chip" :
Millimeter size devices perform laboratory functions relevant to chemistry and biology technology. In these digital microfluidics problems, tiny discrete droplets of liquid, on the order of a picoliter, are transported, mixed, stored, or otherwise manipulated in polymer fluid channels. A process called *flow focusing employs the Rayleigh-Plateau instability in more efficient mixing* processes.

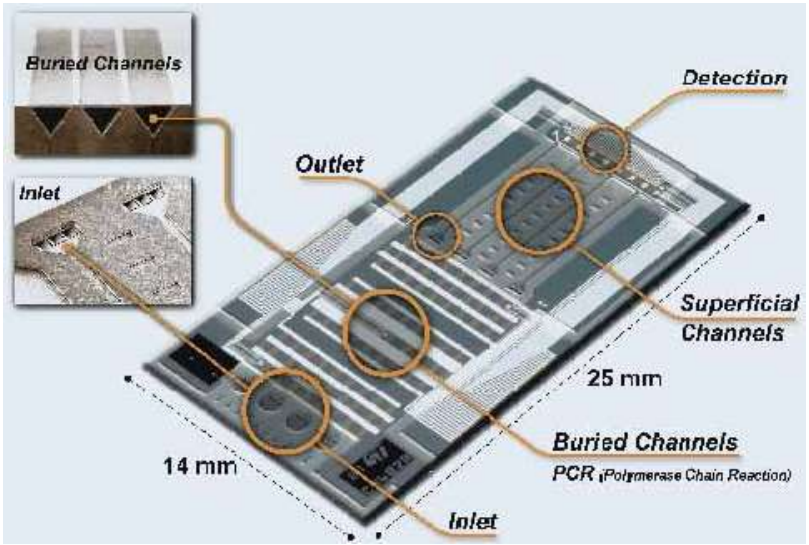


techon.nikkeibp.co.jp

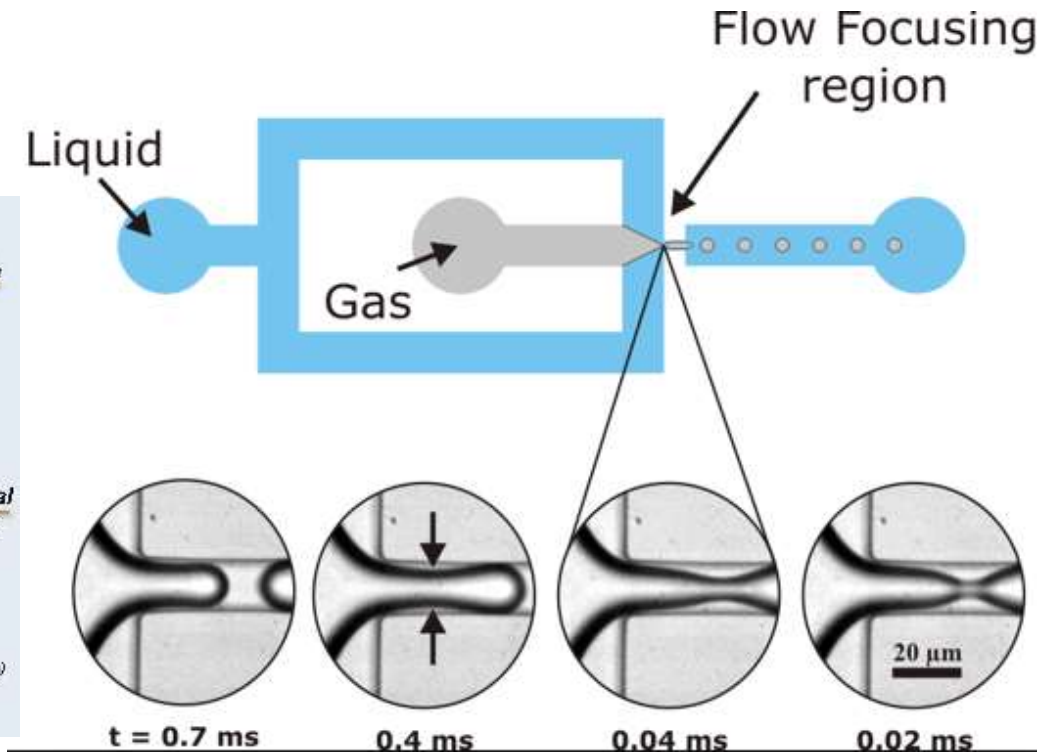


pof.tnw.utwente.nl

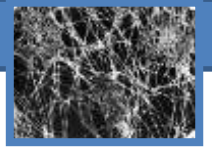

## Rozměrová analýza

The Rayleigh-Plateau instability is defined by two factors:

1. the growth rate of the perturbations and
2. length scale over which the instability grows.


In this system, the time scale is equal to the length scale divided by the jet speed.

The length scale, shown in Fig 2, is the length over which the fluid begins to decompose into droplets. The growth rate of the perturbations is important because it characterizes what disturbances initiate the instability.

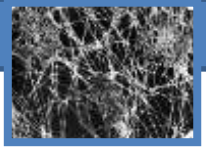

As shown in the next section, the disturbances are a set of sinusoids with varying growth rates and wavenumbers.

Only a limited number of which are unstable.

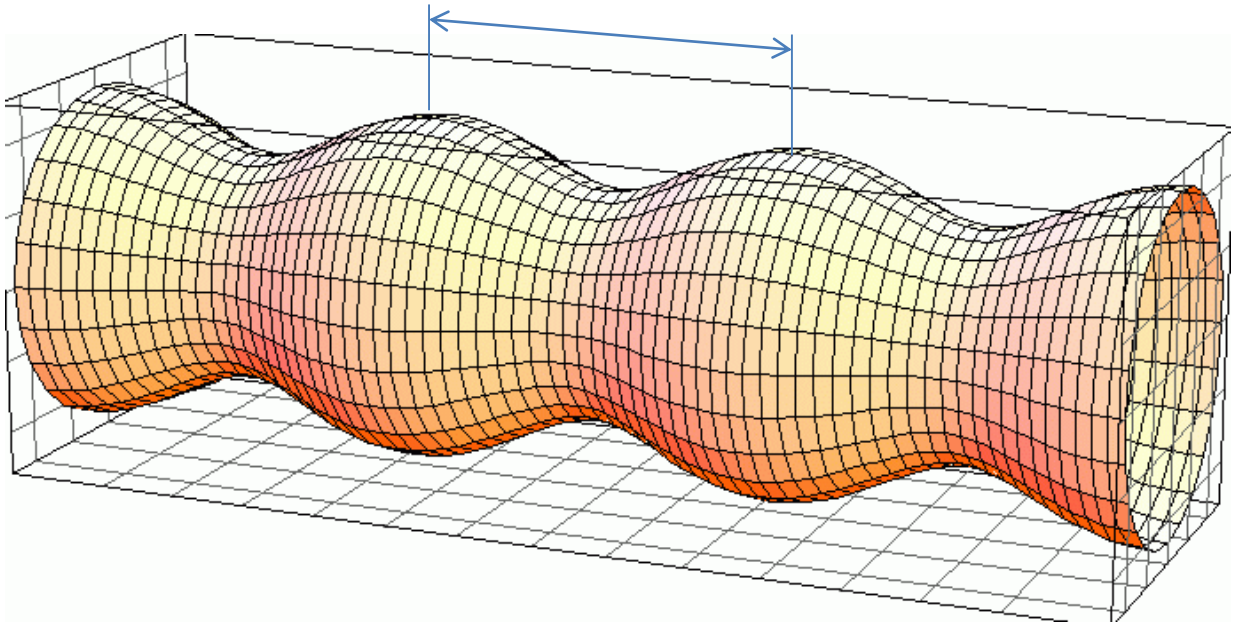

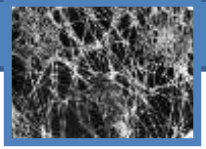

# No-viscosity

$L_{crit}$ je délka nepřerušeného kapalinového sloupce od otvoru zvlákňovací trysky.
$U$ je rychlost (pro zjednodušení konstantní) postupu kapalinového válce.

First, dimensional analysis to find a relationship between the critical length, $L_{crit}$ , and fluid properties.

$$L_{crit} = f\left(\rho, R, U_{jet}, \gamma\right) \qquad (1)$$

where $\rho$, R, $U_{jet}$,$\gamma$ are density, column radius, jet stream velocity, and surface tension, respectively.

One can comprehensively describe the system in terms of energy, with surface tension and momentum flux dominating the system (body forces are negligible).

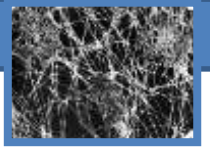

## No-viscosity

The critical length, $L_{crit}$, is normalized by the column radius, $R$.

$$\tilde{L} = \frac{L_{crit}}{R}$$

*The velocity exponent is set to be one. The* resulting equation becomes: $\frac{L}{R} \approx U^1 R^a \rho^b \gamma^c = \left[\frac{L}{T}\right][L]^a \left[\frac{M}{L^3}\right]^b \left[\frac{M}{T^2}\right]^c$

Bezrozměrová veličina

$$\begin{aligned} L: &\quad 1 + a - 3b = 0 \Rightarrow \quad a = 1/2 \\ M: &\quad b + c = 0 \Rightarrow \quad\quad b = 1/2 \\ T: &\quad -1 - 2c = 0 \Rightarrow \quad c = -1/2 \end{aligned}$$

$$\frac{L}{R} \approx U^1 R^{1/2} \rho^{1/2} \gamma^{-1/2} = U\left(\frac{R\rho}{\gamma}\right)^{1/2}$$

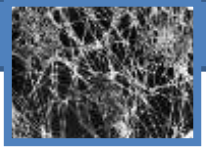

## No-viscosity

$$\frac{L}{R} \approx U^1 R^{1/2} \rho^{1/2} \gamma^{-1/2} = U\left(\frac{R\rho}{\gamma}\right)^{1/2}$$

There appears a critical time scale, also present in the dispersion relation below.

$$\frac{L}{U} = t \approx \left(\frac{R^3 \rho}{\gamma}\right)^{1/2}$$

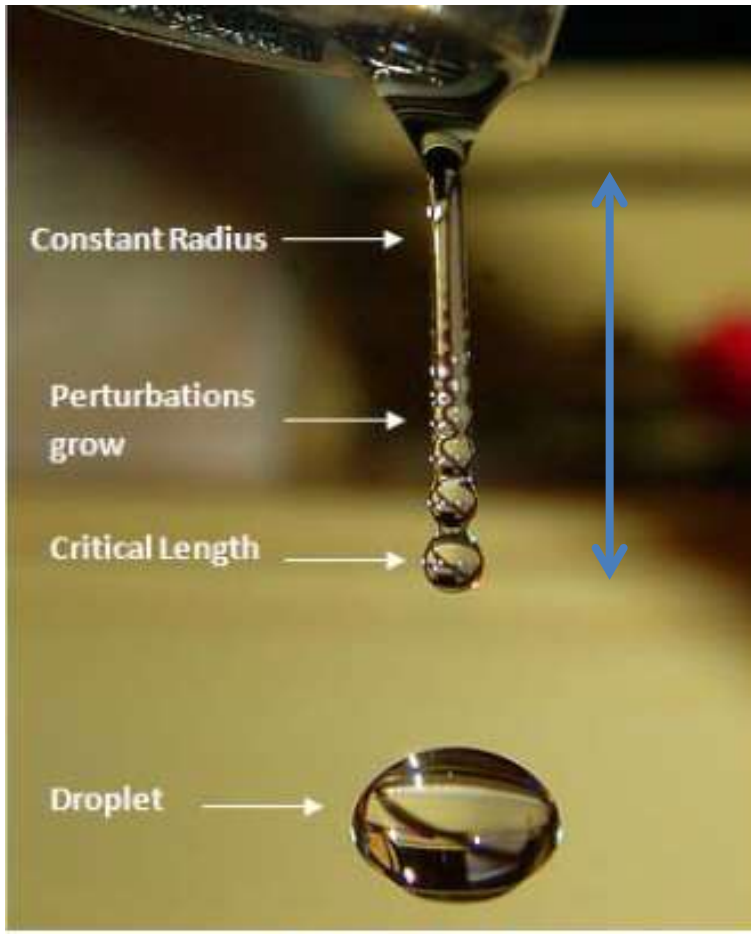


Figure 2: Picture of instability

Veličiny $L_{crit}$, $U$, $t$ se vztahují k tomuto úseku, kdy je kapalinový sloupec kompaktní.

## Viscosity

$$\tau = 5\frac{R\nu\rho}{\gamma}$$

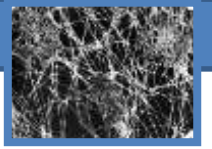

Low-viscosity

$$\tau = 5\frac{R\nu\rho}{\gamma}$$

$$\nu = \frac{\eta}{\rho} = \left[\frac{L^2}{T}\right]$$

$$L_{crit} = f\left(\rho, R, U_{jet}, \gamma, \nu\right)$$

$$\frac{L}{R} \approx U^1 R^a \rho^b \gamma^c \nu^e = \left[\frac{L}{T}\right][L]^a \left[\frac{M}{L^3}\right]^b \left[\frac{M}{T^2}\right]^c \left[\frac{L^2}{T}\right]^e$$

$$L: \quad 1 + a - 3b + 2e = 0 \Rightarrow \quad a = 1/2$$

$$M: \quad b + c = 0 \Rightarrow \qquad b = 1/2$$

$$T: \quad -1 - 2c - e = 0 \Rightarrow \qquad c = -1/2$$

Podurčený systém lineárních algebraických rovnic.

$$L \approx R\frac{\nu}{\gamma}(\rho U)$$

Teorie zvlákňování

$$\tau = \frac{L}{U} \approx R\frac{\nu\rho}{\gamma}$$

Předpoklad lineární závislosti $\tau$ na $\nu$ v případě nízko-viskózních kapalin. Tedy e=1. Odtud plyne: c=1, b=1, a=0

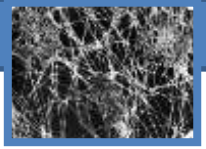

Přehled hodnot dynamických viskozit pro různé kapaliny (při 20 °C)

| **Látka** | **Viskozita *Nsm$^{-2}$*** |
|---|---|
| voda | 0,001 |
| benzín | 0,00053 |
| etanol (líh) | 0,0012 |
| glycerín | 1,48 |
| olej | 0,00149 |

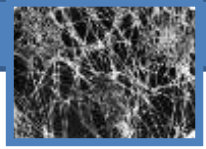

# Kinematická viskozita kapalin při 18 °C

| Látka | Kinematická viskozita υ ($m^2/s$) |
|---|---|
| voda | $1{,}06.10^{-6}$ |
| benzen | $7{,}65.10^{-6}$ |
| benzín | $7{,}65.10^{-7}$ |
| glycerín | $1{,}314.10^{-3}$ |
| chloroform | $3{,}89.10^{-6}$ |
| nitrobenzen | $1{,}72.10^{-5}$ |
| topný olej | $5{,}2.10^{-5}$ |
| motorový olej | $9{,}4.10^{-5}$ |
| rtuť | $1{,}16.10^{-7}$ |
| petrolej | $2{,}06.10^{-6}$ |

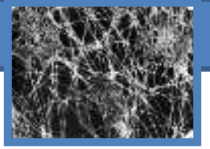

## Kvantitativní popis P-R nestability

$$p_c = \gamma\left(\frac{1}{R_1} + \frac{1}{R_2}\right)$$

$$\frac{1}{R_1} = \frac{1}{R+\varsigma} \cong \frac{1}{R} + \frac{\varsigma}{R^2}$$

$$\frac{1}{R_2} = \frac{\partial^2 \zeta}{\partial x^2}$$

$$p_c = \gamma\left(\frac{1}{R} - \frac{\varsigma}{R^2} - \frac{\partial^2 \varsigma}{\partial x^2}\right)$$

$$\varsigma = A\cos(kx)$$

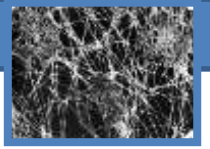

$$p_{c1} = \gamma\left(\frac{1}{R} - \frac{\varsigma}{R^2} - \frac{\partial^2 \varsigma}{\partial x^2}\right) \qquad p_{c0} = \gamma\left(\frac{1}{R}\right)$$

$$p_{c1} - p_{c0} = \gamma\left(-\frac{\varsigma}{R^2} - \frac{\partial^2 \varsigma}{\partial x^2}\right) < 0$$

$$\varsigma = A\cos(kx)$$

$$-\frac{A\cos(kx)}{R^2} + Ak^2\cos(kx) < 0$$

$$k^2 < \frac{1}{R^2}$$

$$2\pi r < \lambda$$

Plateau result

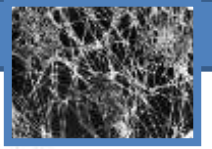

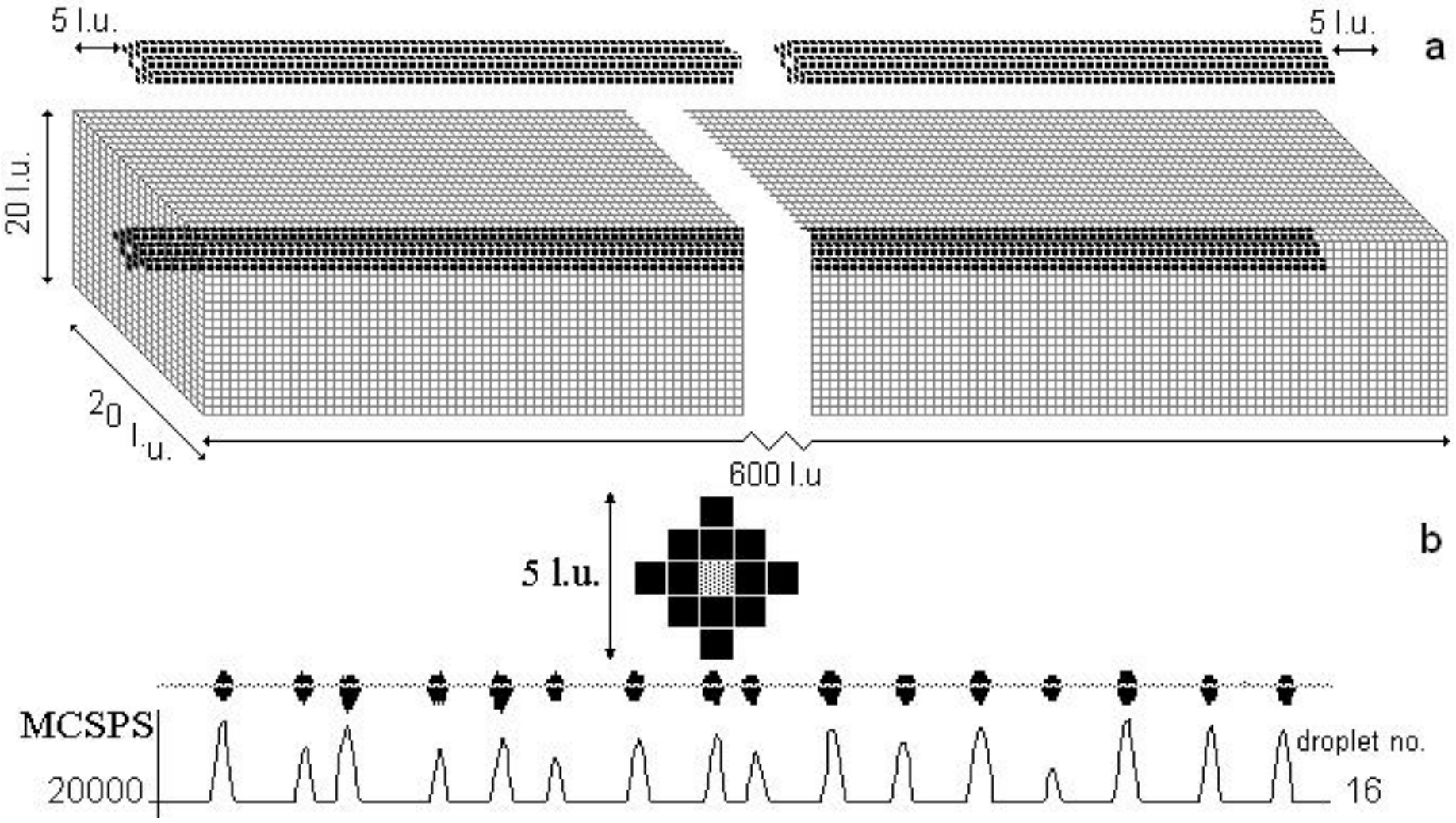


**Fig. 2.** (a) The original longitudinal and cross sectional configurations of the liquid coated fibre; the cubical simulation box of lattice-nodes has dimensions of $N = N_X \times N_Y \times N_Z = 600$ l.u. $\times$ 20 l.u. $\times$ 20 l.u. $= 24 \times 10^4$ (l.u.)$^3$. (b) Detailed cross sectional shape of the original liquid layer on a fibre and the liquid nodes distribution along the fibre axis after the detachment into individual unduloids at the time of MCSPS=20,000.

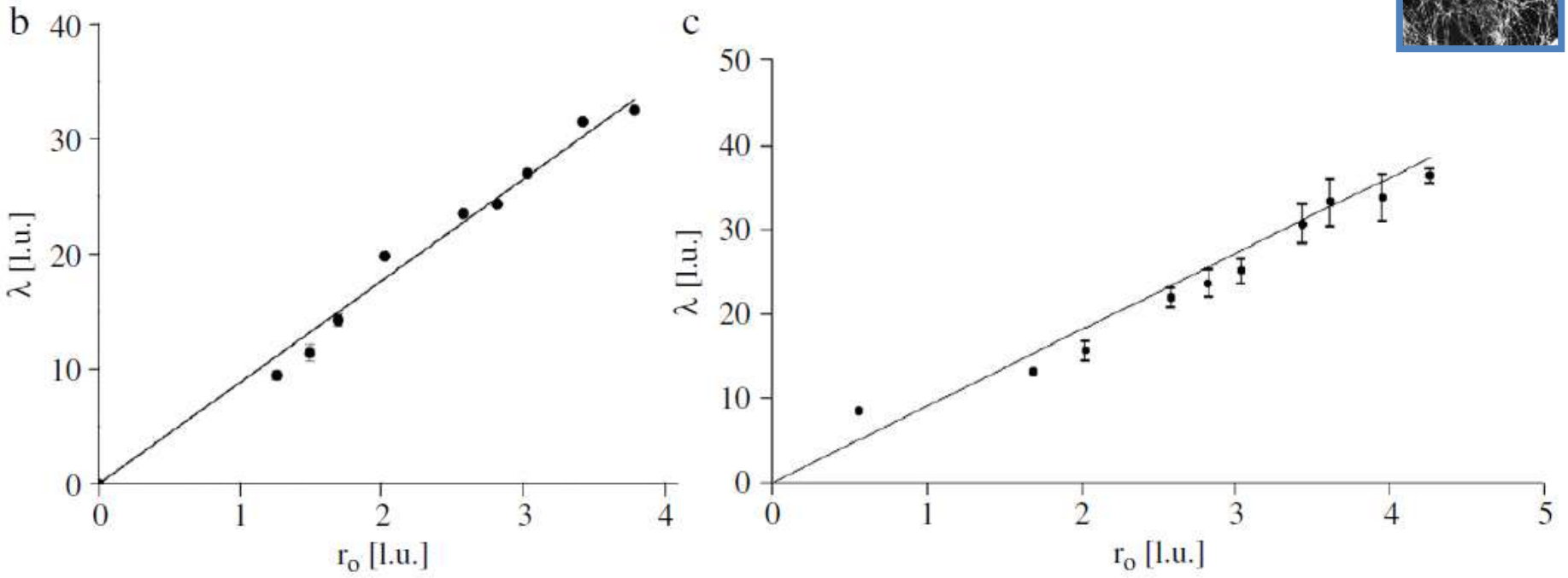


Fig. 5. The Rayleigh wavelength versus the original radius $r_o$ as predicted by the analytical theory, i.e. $\lambda = 2.87\pi\, r_0$, (solid line) and our computer simulations (points) are plotted in parts (b) and (c); (b) is for pure liquid jet and (c) for liquid coating a fibre.

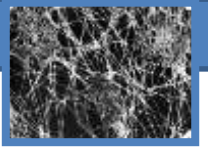

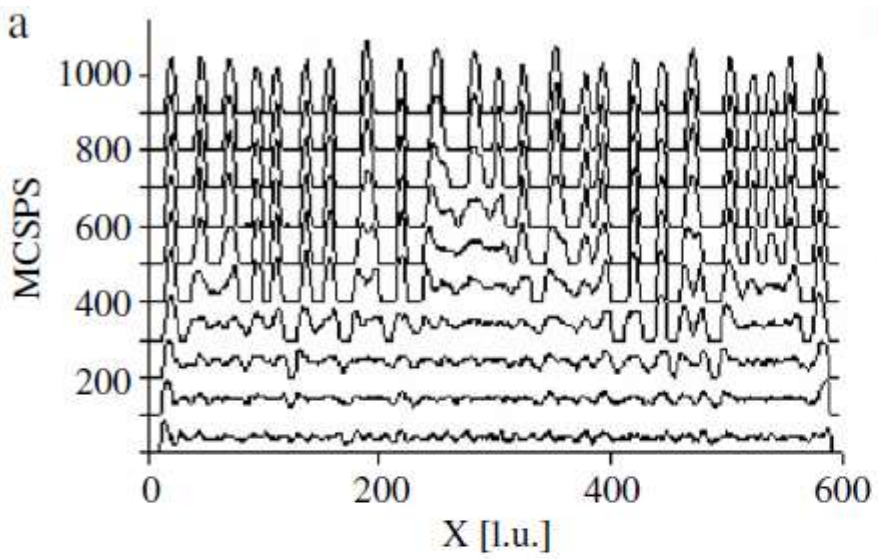


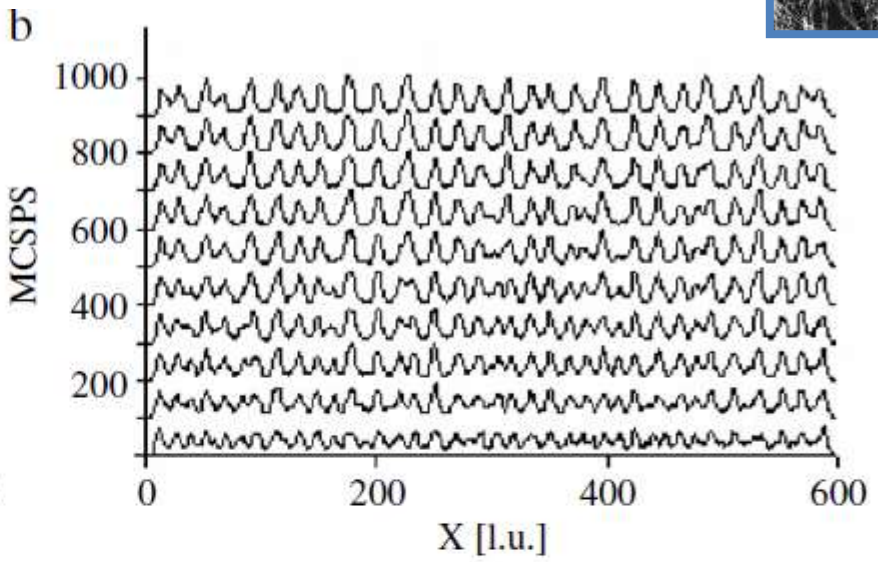


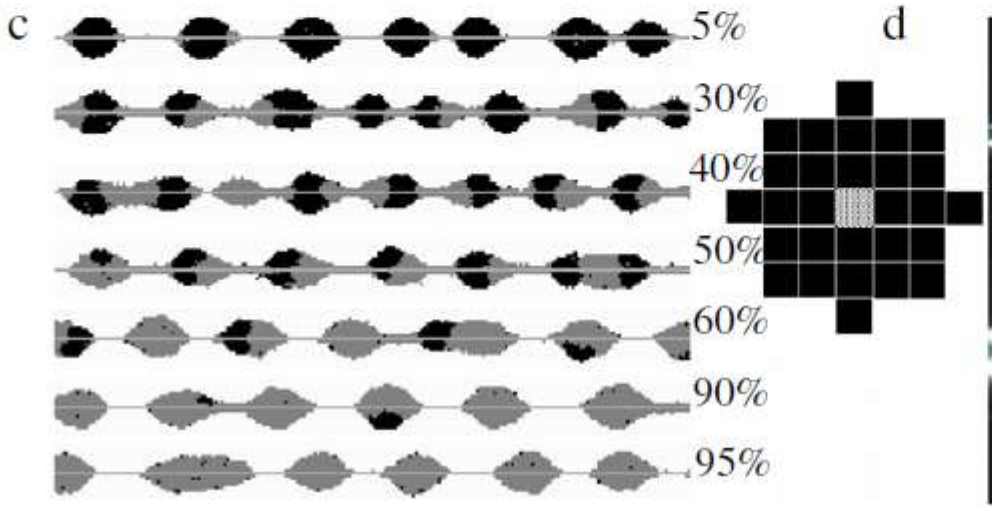


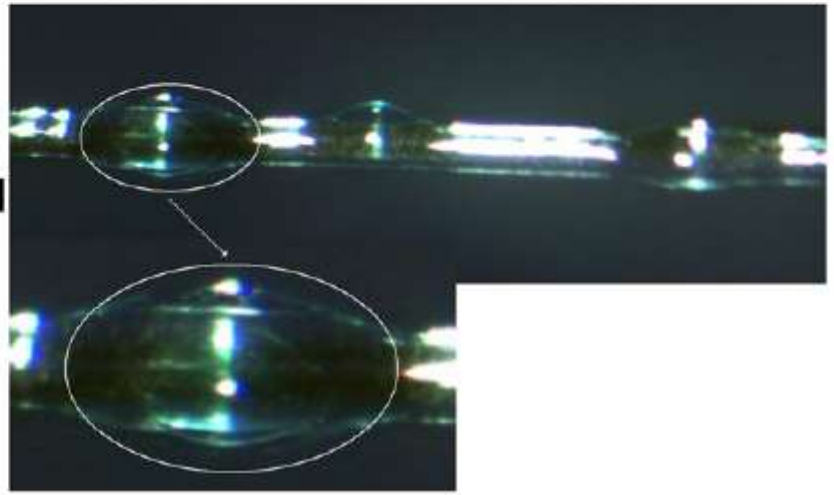


**Fig. 8.** The effect of the concentration of liquid $L_2$ on the temporal evolution of number of droplets. (a) The time development of the system with liquid $L_1$ only. (b) The time development of the system with the 40% of the liquid $L_2$. (c) The computer simulation output for the mixed liquid where the concentration of the liquid $L_2$ varies from 5% up to 95%. (d) A real system composed of a mixture of water and oil.

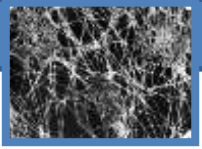

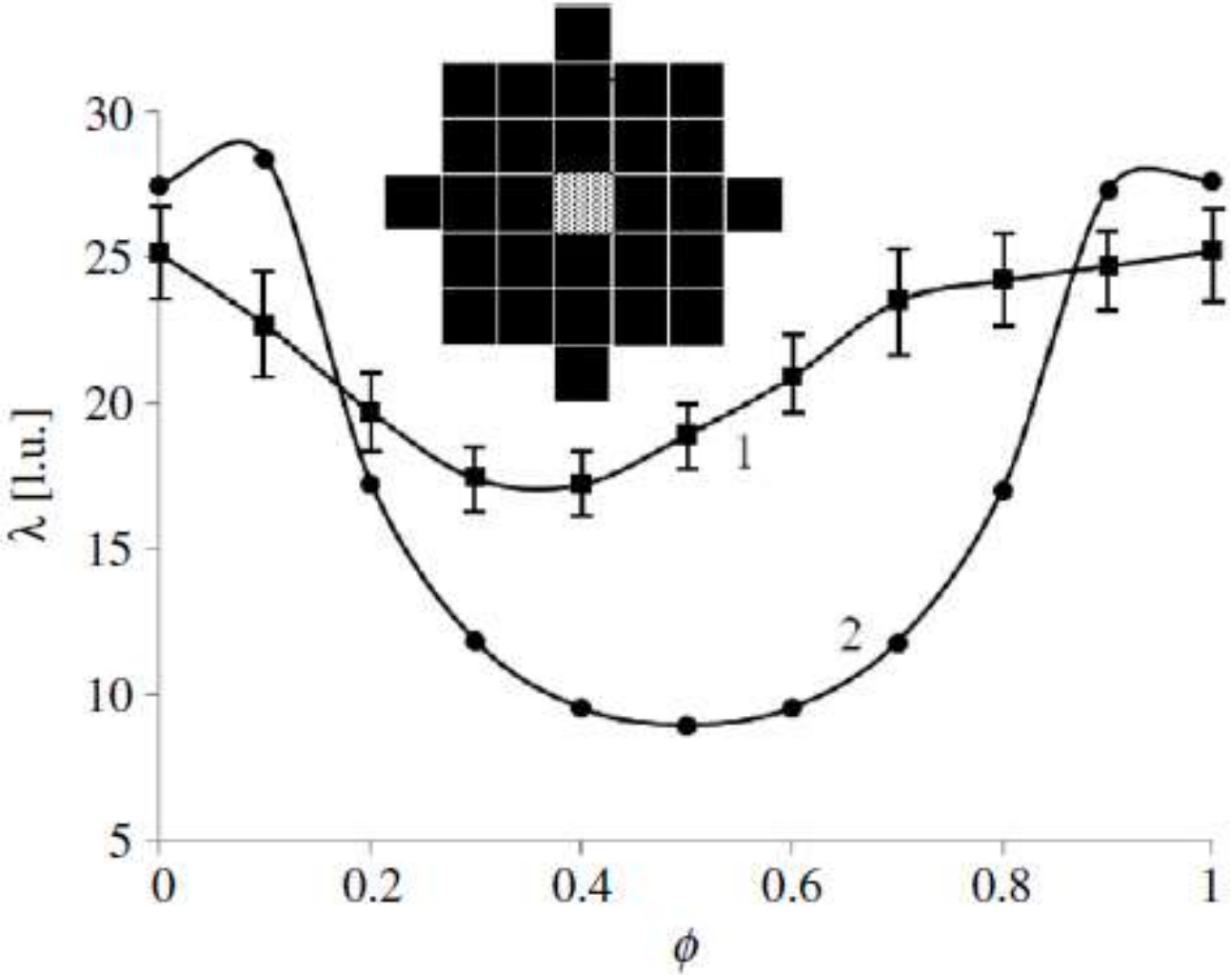


**Fig. 7.** Rayleigh wavelength, $\lambda$, versus the concentration, $\phi$, of the liquid $L_2$ in the liquid $L_1$ for the disintegration process of the immiscible liquids film on a fibre. The curve (1) belongs to the computer simulation, while the dependence (2) represents an estimation provided by the theoretical approach, using Eq. (26).

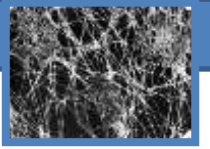

Kvantitativní popis P-R nestability

(2009)'Physical principles of electrospinning (Electrospinning as a nano-scale technology of the twentyfirst century)',*Textile Progress*, 41:2,59 — 140

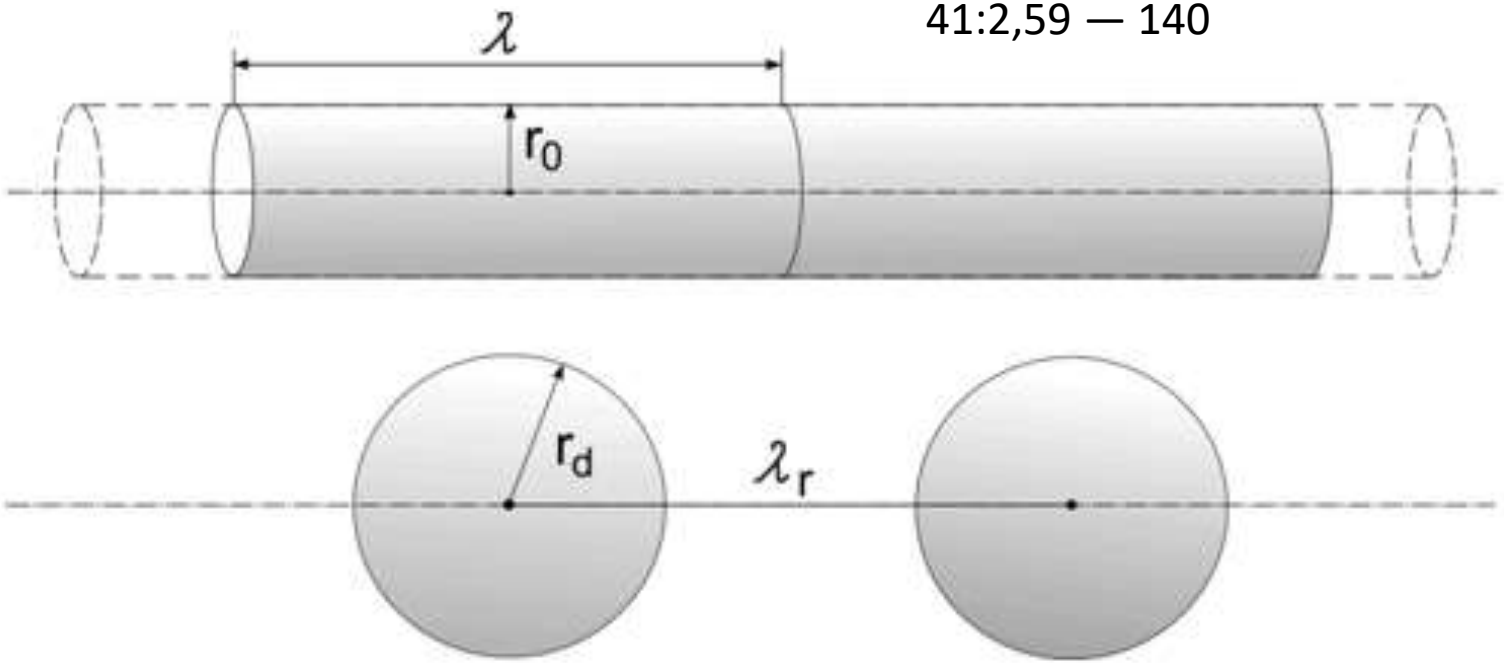


*Figure 4.1. Rayleigh instability: A piece of liquid cylinder with the radius  having length  is equivalent, with respect to volume, to a sphere of the radius . The parameter  is the characteristic distance between droplets into which the liquid cylinder disintegrates.*

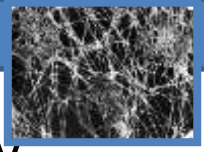

A rough analysis of the Rayleigh instability can be conducted by associating the initial shape of a jet of an incompressible liquid, i.e. a cylinder in the present case, with the final shape of a chain of spherical droplets. The volume conservation between the cylinder and the sphere is assumed and hence holds

$$\pi r_o^2 \lambda = \frac{4}{3} \pi r_d^3$$

where,  is the length of the cylinder  with original radius, $r_o$, that is converted into one droplet of radius, $r_d$, as shown in (Figure 4.1). Rearrangement of the previous relation in terms of droplet radius  causes it to take the following form .

$$r_d = \sqrt[3]{3/4\left(r_o^2 \lambda\right)}$$

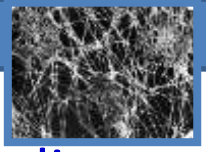

$$2\pi r_0 \lambda \gamma \geq 4\pi {r_d}^2 \gamma$$

$$r_0 \lambda \geq 2{r_d}^2$$

$$\lambda \geq 2\frac{{r_d}^2}{r_0}$$

The surface energy of liquid bodies in spherical or cylindrical form is composed the surface energy.

$$r_d = \sqrt[3]{\frac{3}{4}\left({r_o}^2 \lambda\right)}$$

$$\lambda \geq 2\frac{(3/4)^{2/3}\lambda^{2/3} r_0^{4/3}}{r_0}$$

$$\lambda^{1/3} \geq 2\left(\frac{3}{4}\right)^{2/3} r_0^{1/3}$$

$$\boxed{\lambda} \geq 2^3\left(\frac{3}{4}\right)^2 r_0 = \frac{9}{2} r_0 = \boxed{1.43 \cdot \pi r_0}$$

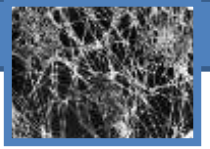

The total energy of liquid bodies in spherical or cylindrical form is composed of two components. Firstly, one is associated with the surface tension $\gamma$, i.e. the surface energy, while the last one is associated with the capillary pressure $p_c$.

$$p_c = \gamma\left(\frac{1}{R_1} + \frac{1}{R_2}\right)$$

$$2\pi r_0 \lambda_e \gamma + \pi r_o \lambda_e \gamma \geq 4\pi {r_d}^2 \gamma + \frac{8}{3}\pi {r_d}^2 \gamma$$

$$\boxed{\lambda_e} \geq \frac{5^3 4}{3^4} r_0 \approx \boxed{1.96\,\pi r_o}$$

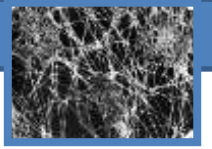

# V) Linear stability analysis

D. Lukas, N. Pan, A. Sarkar, M. Weng, J. Chaloupek, E. Kostakova, L. Ocheretna, P. Mikesa, M. Pociute, E. Amlerf, *Physica A*, 389 (2010) 2164-2176.

$$\omega^2 = \frac{\gamma}{\rho r_0^3} \frac{I_1(kr_0)}{I_0(kr_0)} k r_0 \left(1 - k^2 r_0^2\right)$$

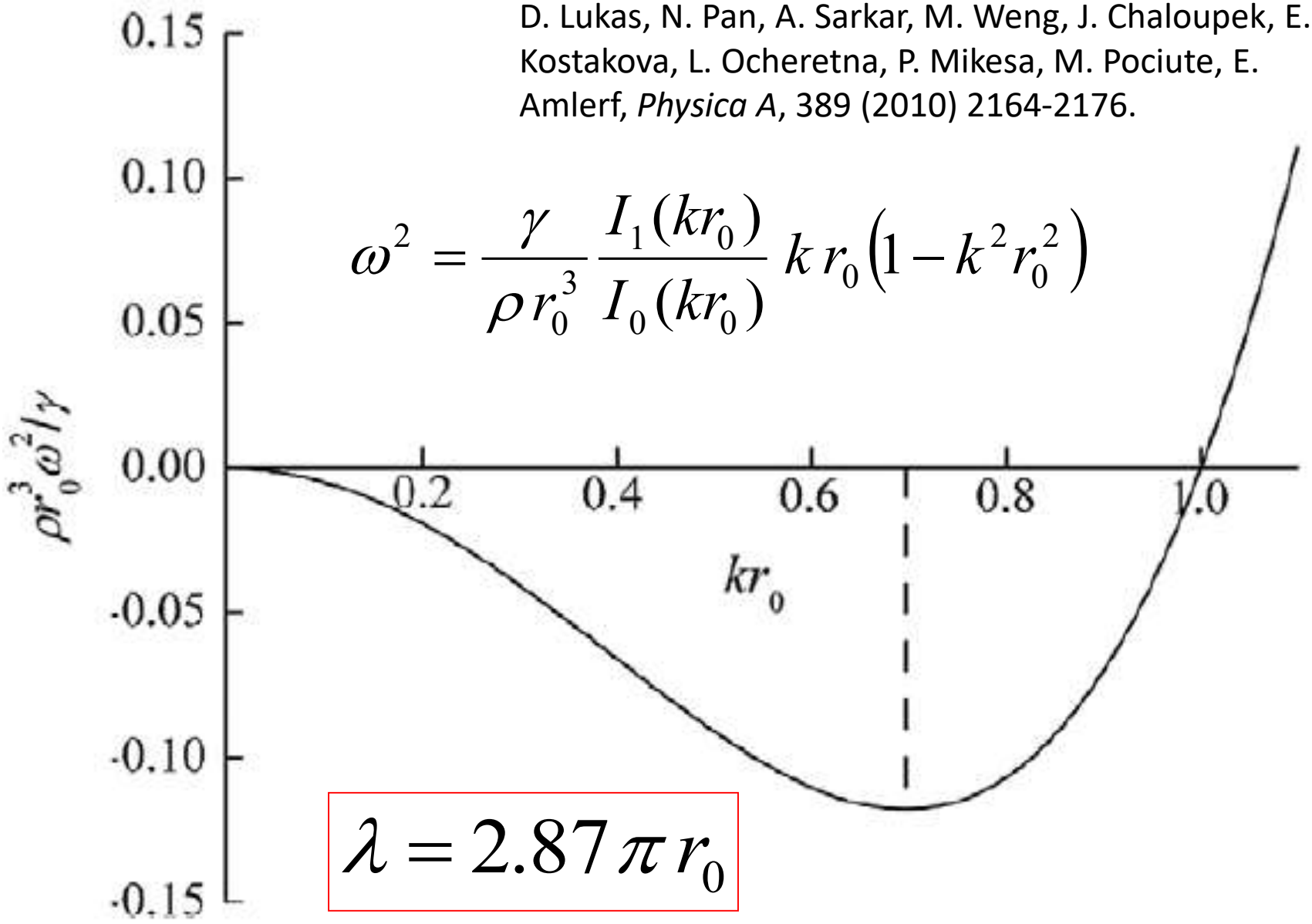


$$\lambda = 2.87 \pi r_0$$